

# EXPERIMENTAL INVESTIGATION OF THE COMBUSTION OF NATURAL GAS/HYDROGEN MIXTURES IN A NOVEL LABORATORY COMBUSTOR

M. Silva, G. P. Pacheco, M. A. A. Mendes and P. J. Coelho

pedro.coelho@tecnico.ulisboa.pt

IDMEC, Mech. Eng. Dept., Instituto Superior Técnico, Universidade de Lisboa

## Abstract

The combustion of natural gas/hydrogen mixtures is experimentally investigated in a laboratory-scale combustor. A distinctive feature of this combustor is the injection of secondary air through holes in a plenum located at the top of the combustor in a direction opposite to the fuel jet, which is supplied along with the primary air through a swirl burner operating at a constant thermal power of 5 kW. The influence of the fuel composition (0% - 100% vol. H<sub>2</sub> in the mixture), excess air coefficient ( $\lambda=1.3-1.7$ ) and primary air percentage ( $\alpha=50\%-100\%$ ) on the temperature and flue gas composition was investigated. The experiments were performed using thermocouples and gas analysers. The results show that the increase of the hydrogen in the mixture, for fixed excess air and primary air percentage, has a relatively small influence on the temperature when the hydrogen content in the fuel ranges from 0 to 80% (vol.) but a greater impact when pure hydrogen is burnt. At  $\lambda=1.3$ , CO emissions are excessively high when secondary air is used, indicating incomplete combustion, but decrease with higher excess air, reduced secondary air, or hydrogen content above 20%. At  $\lambda=1.3$ , NO<sub>x</sub> emissions increase with hydrogen content, decrease slightly as  $\alpha$  rises from 50 to 66.7%, but increase for  $\alpha=100\%$ , reaching a peak for pure hydrogen. At higher excess air coefficients, NO<sub>x</sub> emissions vary weakly up to 80% hydrogen but rise for pure hydrogen, staying below 50 ppm. Secondary air reduces NO<sub>x</sub> emissions but increases CO emissions, making it effective only if the excess air keeps CO emissions within acceptable limits.

## Introduction

The growing need to mitigate climate change, comply with increasingly stringent pollutant emission regulations, and meet rising energy demands has driven the development of renewable energy technologies and accelerated the electrification of various energy sectors. However, despite this shift in the energy paradigm, the decarbonisation process remains relatively slow. In 2023, renewable energy, including traditional biomass, accounted for only 15% of the global energy supply, with fossil fuels still dominating at 80%, and the remaining share supplied by nuclear energy [1]. Moreover, the electrification of certain sectors, such as heavy industry, maritime and air transport, remains challenging. As a result, combustion continues to be a critical technology for meeting energy demand, although its role is expected to diminish over the coming decades. While coal and fuel oil were the dominant fuels in recent decades, their high pollutant emissions have led to a growing shift towards the use of natural gas and alternative fuels.

In this context, hydrogen is considered one of the most promising options for the future [2]. While hydrogen is the most abundant chemical element in the universe, its highly reactive nature means it is always bound to other substances on Earth. As a result, the production, distribution, storage, and utilization of hydrogen are the focus of ongoing, intensive research [3]. Hydrogen combustion offers several advantages over natural gas, including the absence of emissions such as unburnt hydrocarbons, CO, and CO<sub>2</sub>. Additionally, hydrogen has a high energy density per unit mass and a broad flammability range, providing greater flexibility in

combustion applications. However, the use of hydrogen as a fuel presents several challenges, including the lack of a dedicated infrastructure for its transportation, distribution, and storage [4]. Safety concerns, such as the risk of flashback in premixed combustion systems, also need to be addressed [5]. Additionally, hydrogen's unique properties, such as its high laminar flame speed, short ignition delay time, and higher adiabatic flame temperature compared to hydrocarbons, can impact combustion systems and potentially lead to increased NO<sub>x</sub> emissions [6, 7].

The use of pure hydrogen as a fuel remains technologically and logistically challenging. As a transitional solution, hydrogen-enriched natural gas offers an interesting alternative and viable option to gradually facilitate the integration of hydrogen into combustion systems [8]. In fact, the injection of hydrogen at concentrations of up to 20% by volume has already been demonstrated as feasible in existing natural gas infrastructure [9]. Moreover, natural gas cooktop burners can operate safely and efficiently blending up to 20% H<sub>2</sub> with natural gas [10]. In addition, the combustion of hydrogen or mixtures of natural gas and hydrogen with a high hydrogen content are the subject of intensive research.

Flame stabilization in combustion chambers is often achieved using a swirl burner. Several works addressing the combustion of natural gas/hydrogen mixtures using swirl burners have been reported, for both unconfined [11–12] and confined [13–20] flames. Kim *et al.* [11] experimentally investigated the effect of hydrogen addition in methane–air premixed flames for a swirl-stabilized laboratory-scale combustor operated at 5.81 kW under unconfined flame conditions. They studied the combustion characteristics at fixed thermal load but different swirl strengths. Kashir *et al.* [12] performed numerical simulations of a bluff-body stabilized swirling flow burner (Sydney swirl burner). The effect of hydrogen content of blended CH<sub>4</sub>-H<sub>2</sub> flames was investigated for three different swirl numbers.

Lean premixed combustion is a technology often used in gas turbine combustors, industrial burners, boilers and other combustion systems due to its advantages, such as lower combustion temperatures, improved combustion efficiency, and reduced NO<sub>x</sub> emissions. Combustion of hydrogen-enriched methane in a lean premixed swirl-stabilized burner was experimentally and computationally investigated by Schefer *et al.* [13]. They reported a reduction in CO concentration with hydrogen addition, without adversely affecting the NO<sub>x</sub> emissions. Kim *et al.* [14] extended their previous work [11] by confining the flame. They found that the addition of hydrogen raises the peak temperature, leading to increased NO<sub>x</sub> formation rate in the reaction zone and higher NO emissions. However, this effect could be mitigated by increasing the excess air or enhancing the swirl intensity. The influence of the swirl was also explored by Du *et al.* [15] for premixed combustion of hydrogen-blended natural gas in a swirl burner. They concluded that CO and NO emissions gradually decrease and combustion performance improved when the swirl angle is set to 45°. Another recent computational investigation of the influence of the swirl intensity on premixed combustion of CH<sub>4</sub>-H<sub>2</sub> mixtures in a swirl combustor was reported in reference [16]. It was found that increasing the swirl intensity leads to an increase of the size of the inner recirculation zone, a shorter flame and a higher temperature. The influence of hydrogen content in the fuel and equivalence ratio was also addressed.

Non-premixed combustion of natural gas/hydrogen mixtures in swirl burner combustors has also been the subject of research. Cozzi and Coghe [17] studied the combustion of fuel mixtures containing 0% up to 100% hydrogen in a co-flow configuration. They reported that hydrogen addition yields a shorter flame located closer to the burner head and a monotonic increase of both CO and NO<sub>x</sub> emissions in the range 0%-80% H<sub>2</sub>. An experimental and numerical work focused on the non-premixed combustion characteristics and emissions of hydrogen-enriched methane under ultra-lean conditions was performed by Mokheimer *et al.* [18]. The maximum temperature of the combustor and the residence time of combustion

products were found to be the key factors influencing  $\text{NO}_x$  emissions. Higher  $\text{NO}_x$  emissions were observed at higher equivalence ratios and/or greater hydrogen content in the fuel mixture. Large eddy simulation of an upward swirl can combustor was reported by Rajpara *et al.* [19]. Their results reveal that hydrogen addition to methane increases flame temperature, decreases flame dimensions and reduces CO emissions significantly with a marginal increase in  $\text{NO}_x$  emissions. A scaled industrial low-swirl burner was experimentally studied by Gee *et al.* [20]. Compared to natural gas, hydrogen exhibited a 33% reduction in the radiant fraction and up to a 380% increase in  $\text{NO}_x$  emissions. Daurer *et al.* [21] conducted both experimental and computational studies on an industrial-scale low-swirl burner, operating within a power range of 75–120 kW, and examined natural gas/hydrogen mixtures with hydrogen content ranging from 0% to 100%. Hydrogen enrichment increased furnace temperatures in both experiments and simulations, especially with over 50%  $\text{H}_2$  (vol.) in the fuel.

In this work, an experimental investigation of non-premixed combustion of natural gas/hydrogen mixtures in a swirl burner is reported. The combustor exhibits a unique feature, namely the injection of secondary air from a plenum placed at the top of the combustor in a direction opposite to that of the main flow. The air staging creates a fuel-rich primary combustion zone, which can help reduce  $\text{NO}_x$  emissions, which is a common challenge when burning hydrogen. The effect of the fuel composition, overall excess air coefficient and amount of primary air are examined.

### **Experimental Methodology**

Figure 1 illustrates the combustion chamber used in this study, which consists of a vertical quartz-glass cylinder with an inner diameter of 100 mm, a length of 300 mm, and a thickness of 10 mm. The chamber was wrapped in a 30 mm thick glass-fiber blanket for insulation during the experiments. The burner, positioned centrally, features a central hole surrounded by an annular swirler with vanes angled at  $45^\circ$  to the axial direction. The burner head is raised, resting inside the chamber at a height of 25.8 mm above the base of the quartz-glass, on the top of a truncated cone. The chamber allows for both primary and secondary air injection: primary air is injected through the burner, while secondary air is supplied via a top-mounted plenum that has eight 3 mm diameter holes located at a distance of 2 mm from the chamber's inner wall, as shown in Figure 1. During testing, the primary air and the fuel were injected through the swirler and the burner's central tube, respectively. Although the combustion air is not preheated, heat is transferred from the exhaust gases to the secondary air through the wall of the top piece (labelled '1' in Figure 1) due to the chamber design.

Prior to testing and after ignition, the combustion chamber operated for approximately one hour to reach stable conditions and minimize transient heat losses during the measurements. The fuel mass flow rate was kept constant for all operating conditions to maintain the thermal input (5 kW) unchanged. Temperature and species concentration were measured using probes mounted on a movable arm, inserted through the top of the chamber for precise axial measurements.

Local mean temperatures were measured with 76  $\mu\text{m}$  diameter fine-wire platinum/platinum-13% rhodium (type R) thermocouples. The thermocouple hot junction was supported by 350  $\mu\text{m}$  wires of the same material, encased in a twin-bore alumina sheath with an external diameter of 5 mm. The analog outputs from the thermocouples and analysers were transmitted via A/D boards to a computer for processing. Temperature measurements were taken along the central axis of the combustor ( $r=0$  mm) at various distances from the burner. At each probe position, three measurements, each lasting 10 seconds, were recorded and averaged. The gas temperature data was highly repeatable, with an average temperature standard deviation of 2.2% from the mean.

Gas samples for O<sub>2</sub>, CO<sub>2</sub>, CO, and NO<sub>x</sub> concentration measurements were collected using a stainless-steel, water-cooled probe with a central 1.3 mm diameter sampling tube. This tube was surrounded by two concentric tubes for probe cooling, resulting in an outer diameter of 15 mm. For all test conditions, the gas analyser probe was positioned 300 mm from the base, centred along the chamber's axis. This location was chosen to minimize the probe's impact on flame dynamics, as deeper insertion of the water-cooled probe under certain conditions quenched the flame, leading to unrepresentative gas concentration measurements.

The gas sample was drawn through the probe and part of the system using an oil-free diaphragm pump. To prevent chemical reactions, the sample was rapidly cooled by the high water-cooling rate in the surrounding annulus as it entered the probe's central tube. A condenser removed most particulates and condensate, and a filter and dryer further eliminated any residual particles and moisture, providing clean, dry combustion gases to the analysers. Species concentrations were then recorded on a dry basis, with no attempt to measure fluid flow disturbances caused by the probe.

Table 1 summarizes the characteristics of the gas analyser used. As per the manufacturer's documentation, the analyser has an uncertainty of  $\pm 0.5\%$  of the full scale used, and the reproducibility uncertainty, accounting for the equipment uncertainty and measurement deviation, is less than 5% of the mean value.

The experimental setup includes a natural gas supply from the grid, controlled by an individual mass flow controller. Air at atmospheric pressure is supplied to both primary and secondary air inlets, with mass flow controllers regulating the flow. The air supply was precisely controlled, allowing adjustments from 100% of primary air to 100% of secondary air. The gas species data demonstrated high repeatability and the average standard deviation of the concentration measurements was 5% from the mean.

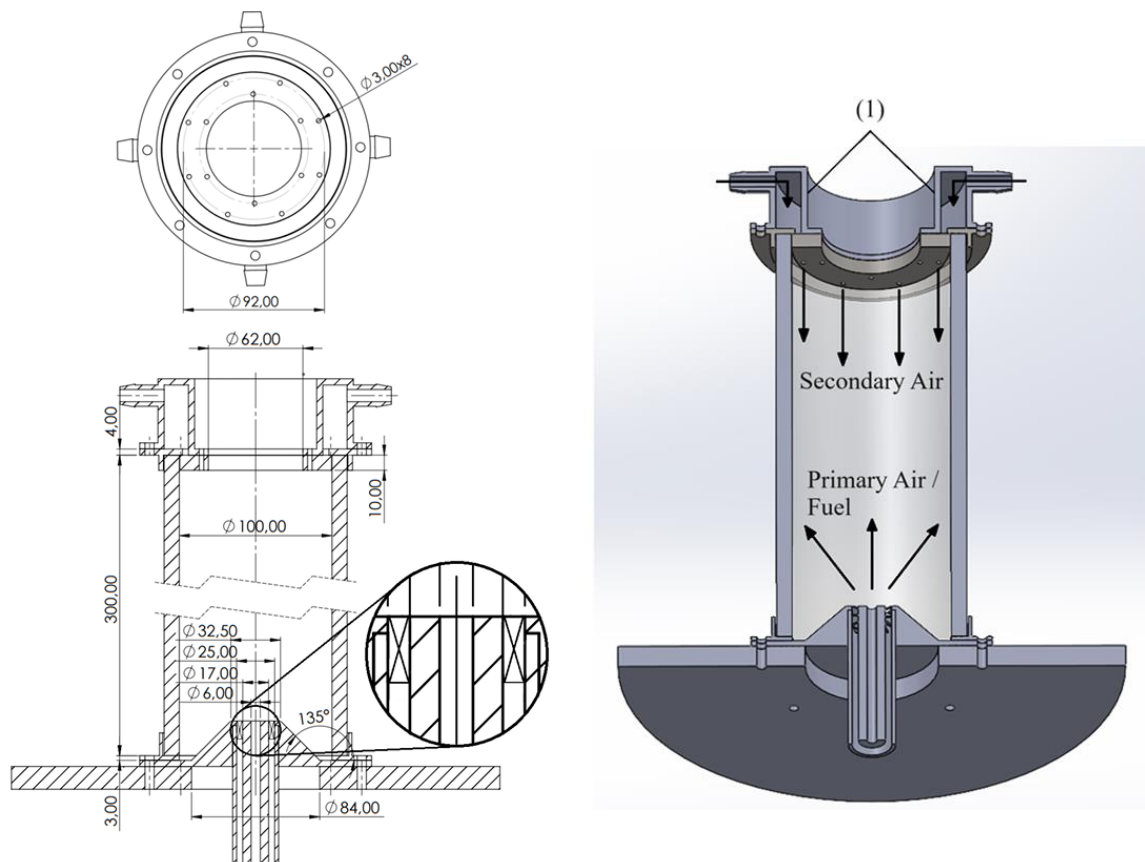


**Figure 1.** Schematic of the combustion chamber.

**Table 1.** Gas analysers characteristics.

Gas Species	Model/Brand	Analysis Method	Value Range
NO <sub>x</sub>	Horiba pg-250	Chemiluminescence	0 – 2500 ppm vol.
O <sub>2</sub>	Horiba CMA-331 A	Paramagnetism	0 – 10 % vol.
CO	Horiba CMA-331 A	Nondispersive	0 – 5000 ppm vol.
CO <sub>2</sub>	Horiba CMA-331 A	Nondispersive	0 – 50 % vol.

## Results and Discussion

In the present work, the volumetric percentage of hydrogen in the fuel ranges from 0 to 100%. The molar mass of hydrogen is approximately one-eighth that of methane. The composition of natural gas varies, depending on its extraction location, but its main component is methane and usually contains small amounts of higher hydrocarbons, carbon dioxide and nitrogen. Accordingly, the molar mass of natural gas is a little higher than that of pure methane. Therefore, at a given temperature, the density of a mixture of natural gas and methane decreases linearly, by a factor of more than eight, when the amount of hydrogen in the mixtures increases from 0 to 100%. Conversely, the lower heating value of the mixture ranges from a little less than 50 MJ/kg for 0% H<sub>2</sub> to 120 MJ/kg for 100% H<sub>2</sub> in the mixture. However, the increase is small up to a large amount of H<sub>2</sub> (e.g., the heating value of the mixture is about 70 MJ/kg for 80% H<sub>2</sub> vol.) and then rises significantly as the percentage of H<sub>2</sub> in the mixture approaches 100%.

In the present work, the thermal power of the combustor is maintained constant and equal to 5 kW. Hence, when the amount of hydrogen in the mixture increases, so do the fuel volumetric flow rate and the fuel velocity at the burner exit. The increase is again more pronounced when the amount of hydrogen in the mixture is high.

Figure 2 shows the temperature profiles along the centreline of the combustor for different values of the volumetric percentage of hydrogen in the fuel, ranging from 20 to 100%. The results are displayed for several values of the overall excess air coefficient ( $\lambda=1.3, 1.5$  and  $1.7$ ) and mass fraction of primary air ( $\alpha=50, 66.7$  and  $100\%$ ). Numerical simulations, which are not presented here, have shown that the momentum of the secondary air jets is not sufficient to allow them to reach the reaction zone downstream of the burner. Therefore, for the considered values of  $\alpha$  and  $\lambda$ , the air/fuel mixture in that reaction zone is rich, except for  $\alpha=100\%$ .

The temperature profiles for natural gas/hydrogen mixtures with 20% to 80% H<sub>2</sub> are relatively close to each other, while the profile for pure hydrogen is clearly distinct, regardless of the values of  $\alpha$  and  $\lambda$ . The increase of the temperature in the vicinity of the burner occurs progressively closer to the burner when the amount of hydrogen in the mixture is reduced, i.e., when the fuel velocity at the burner exit is lower. This suggests that when the percentage of hydrogen in the mixture rises, the increase of the velocity of the fuel exiting the burner prevails over the increased reactivity, thereby shifting downstream the rise of the temperature. Following this sharp rise of temperature, and up to 80% H<sub>2</sub> in the fuel, the temperature continues to increase slowly up to about 18 cm from the burner exit and then either remains approximately constant, as in the case of  $\lambda=1.3$  and  $\alpha=50\%$ , or decreases towards the exit. The peak temperature for pure hydrogen occurs closer to burner and is the highest, because the adiabatic flame temperature of hydrogen is greater than that of methane. The temperature decreases further downstream towards the exit where it reaches values that in most cases are a little lower for 100% H<sub>2</sub> than for natural gas/hydrogen mixtures.

The influence of the excess air on the temperature along the centreline is illustrated in Fig. 3(a) for  $\alpha=50\%$ , considering 20% and 100% H<sub>2</sub> in the fuel. The increase of the overall excess

air implies that there is more air available in the region close to the burner but not enough to fully burn the fuel, i.e., the mixture is rich and approaches stoichiometric conditions. This justifies the faster rise and the slight increase in temperature, leading to higher peak temperature, especially when  $\lambda$  increases from 1.5 to 1.7. Moreover, the higher amount of primary air when  $\lambda$  increases, while maintaining  $\alpha$  constant, leads to enhanced swirl and mixing, which contributes to increase the reaction rates and the temperature. At the exit, the temperature is lower for higher values of  $\lambda$ , as expected.

The effect of the percentage of primary air,  $\alpha$ , on the axial temperature profile is presented in Fig. 3(b) for  $\lambda=1.3$ . Fuels with 20% and 100% H<sub>2</sub> are considered again. The temperature increases faster downstream of the burner when the amount of primary air increases for both fuel compositions. The explanation is identical to that given above when  $\lambda$  increases for

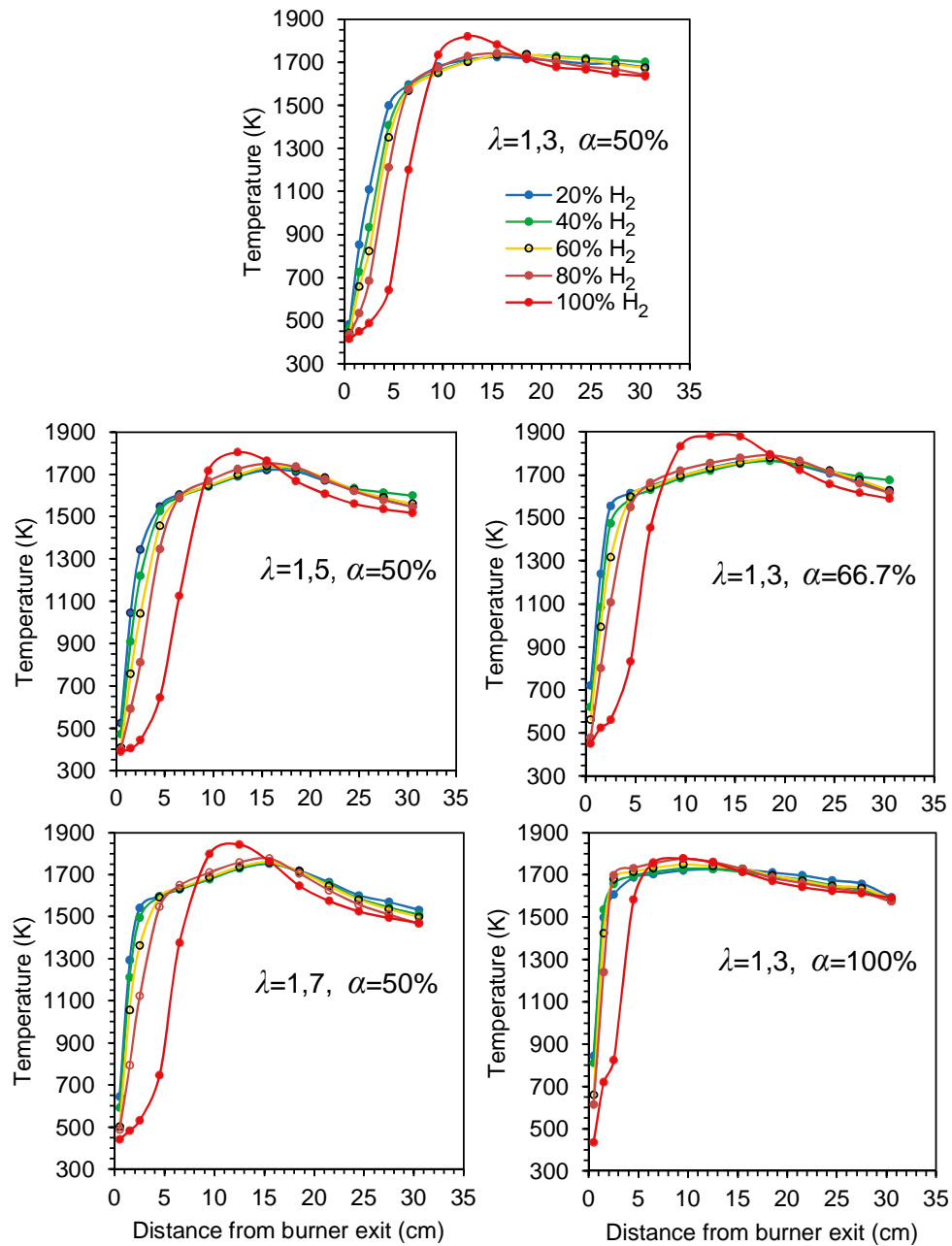


**Figure 2.** Temperature profiles along the centreline – Influence of the excess air coefficient and percentage of hydrogen in the fuel.

constant  $\alpha$ . The peak temperature at the centreline is greater for  $\alpha=66.7\%$  than for  $\alpha=50$  or  $100\%$ . This may be due to the differences between the adiabatic flame temperatures. When only the primary air is considered, the equivalence ratio is equal to 0.77, 1.15 and 1.54 for  $\alpha=50$ , 66.7 and  $100\%$ , respectively, and the corresponding adiabatic flame temperature is higher for  $\alpha=66.7\%$ , and for both 20% and 100%  $H_2$ . In addition, the peak temperature occurs closer to the burner for  $\alpha=100\%$ . This effect may be due to the higher amount of primary air, which promotes the swirl, generating a stronger central recirculation zone, thereby stabilizing the flame closer to the burner and shifting the peak temperature upstream.

The radial temperature profiles at  $x=10$ , 15, and 20 cm downstream of the burner exit are shown in Fig. 4 for  $\lambda=1.3$  and for both 20 and 100%  $H_2$  in the fuel. The temperature is fairly uniform in the combustor for 20%  $H_2$  in the fuel. At  $x=10$  cm, the temperature is a little higher for  $\alpha=66.7\%$ , which is related to the higher adiabatic flame temperature when only the primary air is accounted for. Apart from a temperature increase in the radial direction up to about  $r=2$  cm, for 100%  $H_2$  and for both  $x=50$  and 100 mm, there is a consistent temperature decrease towards the wall of the combustor. This is due both to the heat loss to the wall, that is not fully prevented by the insulation blanket, and the cooling effect of the secondary air. The latter effect is more effective near the combustor exit, due to the decay of the velocity of the secondary air jets as they move away from the injection holes located at the plenum mounted on the top of the combustor.

The molar fractions of  $O_2$ ,  $CO_2$ ,  $CO$  and  $NO_x$  were measured at the exit section of the combustor, both at the centreline and at a distance of 1.5 cm from the centreline. The measurements revealed that while the  $CO_2$  molar fractions are similar at those two locations (maximum difference of about 1%), the  $O_2$ ,  $CO$  and  $NO_x$  molar fractions exhibit larger differences. In the case of  $O_2$ , the molar fraction at the centreline is up to 10% lower than at  $r=1.5$  cm for  $\lambda=1.3$ , but the differences are greatly reduced for higher values of  $\lambda$ . The  $CO$  molar fractions exhibit the largest differences between the two locations, being higher at the centreline. In the case of  $NO_x$ , the difference between the molar fractions at the two positions is typically below 3%.

The experimental data at  $r=1.5$  cm are shown in Fig. 5 for different fuel compositions and for  $\lambda=1.3$ , 1.5 and 1.7, on a dry basis. The percentage of primary air was maintained constant and equal to 50%. The  $O_2$  molar fraction increases with the amount of  $H_2$  in the fuel, for a fixed  $\lambda$ , and increases with  $\lambda$ , for the same fuel, as expected. This trend is not verified for  $\lambda=1.3$  when the percentage of  $H_2$  in the fuel varies from 0% up to 60% but the variation in  $O_2$  emissions is small for these operating conditions. Conversely, the  $CO_2$  and  $CO$  emissions decrease with the increase of  $H_2$  in the fuel, due to the lower amount of carbon available in the fuel, and with the reduction of the excess air coefficient, primarily due to the lower dilution. An exception to this behaviour is observed when the fuel changes from 100% NG to a mixture of 80% NG and 20%  $H_2$ . In this case, an increase of the  $CO$  is observed, as well as a small increase of  $CO_2$  for  $\lambda=1.3$ .

The  $CO$  emissions are unacceptably large for practical applications when  $\lambda=1.3$ , suggesting that combustion is incomplete. However, they decrease significantly with an increase in the excess air coefficient. In fact, the mixture is rich in the region downstream of the combustor since the secondary air jets do not have enough momentum to penetrate and reach that region, according to the numerical simulations mentioned above. The high  $CO$  emissions for  $\lambda=1.3$  suggest that the secondary air mixed with recirculated combustion products is not able to fully burn the remaining fuel and there are still chemical reactions occurring at the exit of the combustor. This explanation is supported by the measurements of the species at the combustor exit, which reveal that the  $O_2$  molar fractions decrease in the radial direction while those of  $CO$  exhibit an opposite trend. The  $NO_x$  emissions increase with the hydrogen content in the fuel at

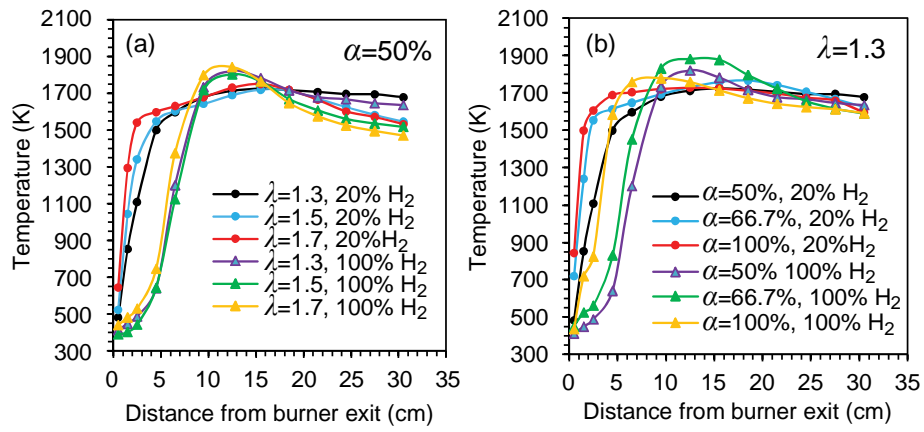


**Figure 3.** Temperature profiles along the centreline: (a) Influence of the percentage of hydrogen in the fuel, (b) Influence of the excess air coefficient

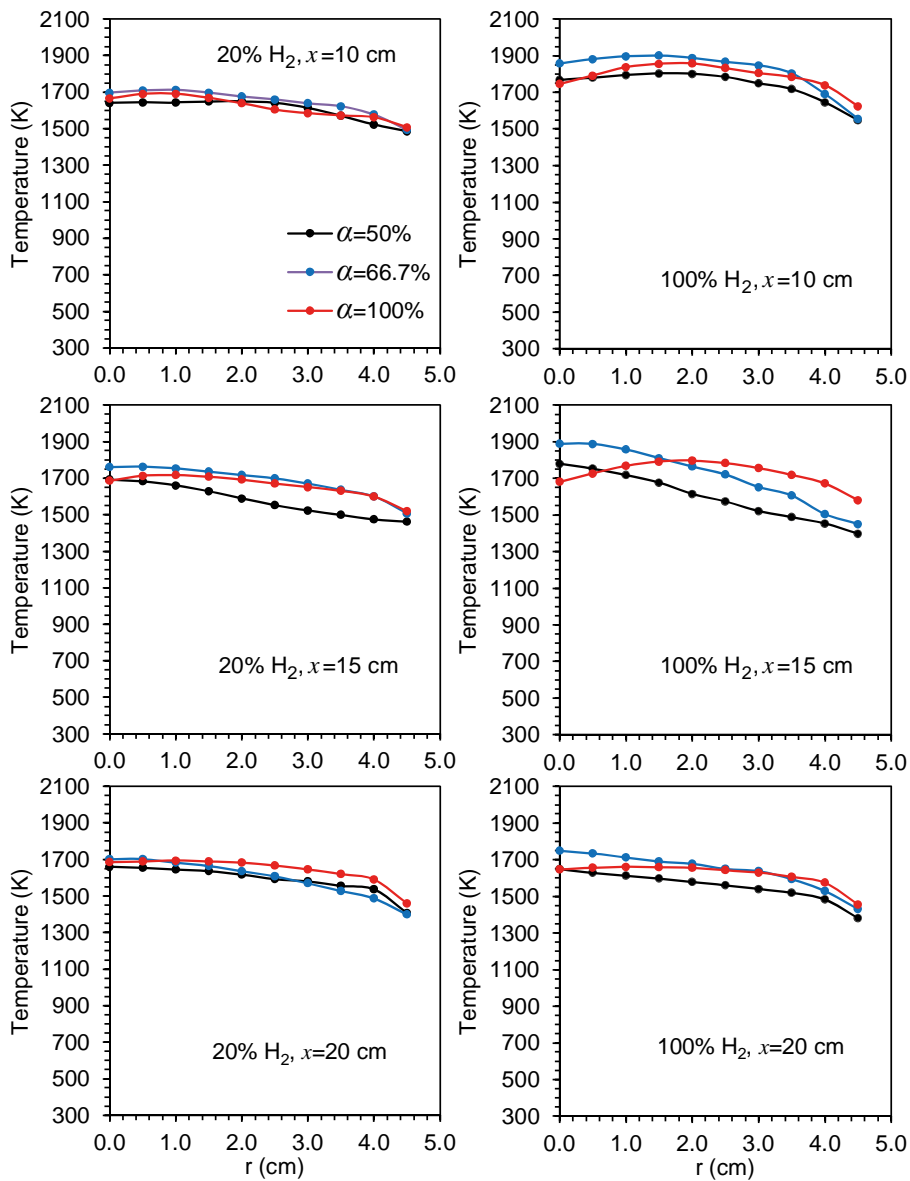


**Figure 4.** Radial temperature profiles for  $\lambda=1.3$  – Influence of the percentage of primary air for 20% and 100%  $\text{H}_2$  in the fuel.

$\lambda=1.3$  but do not exceed 50 ppm. At  $\lambda=1.5$  or 1.7, there is little variation across the 0%–80%  $H_2$  fuel range, and despite a significant increase for pure hydrogen, they remain also below 50 ppm. Although the  $NO_x$  emissions are relatively low, they are not as small as those typically found in the MILD combustion regime.

The influence of the percentage of primary air on the emissions is shown in Fig. 6 for  $\lambda=1.3$ . The  $CO_2$ , CO and  $NO_x$  molar fractions are corrected to a standardized oxygen level of 3% to allow for a consistent comparison of emissions in different combustion systems operating at different excess air coefficients. The variation of the emissions with the fuel composition follows the trends discussed above, i.e., it is independent of  $\alpha$ . Although, for a given fuel composition, the  $O_2$  and  $CO_2$  molar fractions at the exit do not vary much with the percentage of primary air, the  $O_2$  molar fraction tends to be higher and the  $CO_2$  molar fraction lower when there is no secondary air ( $\alpha=100\%$ ), which supports the previous observation of incomplete combustion when secondary air is present. This is confirmed by the CO emissions, which are significant for both  $\alpha=50\%$  and  $\alpha=66.7\%$ . However, in the case of pure hydrogen there is no evidence of incomplete combustion and the  $O_2$  emissions do not vary with  $\alpha$ . The CO emissions are significantly reduced as the percentage of secondary air increases. The  $NO_x$  emissions tend to decrease a little when  $\alpha$  increases from 50 to 66.7% but rise and achieve their highest values of about 100 ppm for  $\alpha=100\%$ . Hence, the secondary air contributes to reduce the  $NO_x$  emissions for pure hydrogen.

According to the Portuguese emission regulations, the maximum CO emission for new gas turbine combustors is  $100 \text{ mg/Nm}^3$  (corrected to 15%  $O_2$ ) for gaseous fuels, including natural gas, which corresponds to about 240 ppm (corrected to 3%  $O_2$ ). In addition, the maximum  $NO_x$  emission for gas turbine combustors is 50 and  $75 \text{ mg/Nm}^3$  (corrected to 15%  $O_2$ ) for natural gas and other gaseous fuels, respectively, which corresponds to 120 and 180 ppm (corrected to 3%  $O_2$ ), respectively. In the case of medium combustion plants with a nominal thermal power in the range 1–50 MW, the maximum  $NO_x$  emission is 100 and  $200 \text{ mg/Nm}^3$  (corrected to 3%  $O_2$ ) for natural gas and other gaseous fuels, respectively, which corresponds to 48.8 and 97.6 ppm (corrected to 3%  $O_2$ ), respectively. However, these limits refer to combustion systems with a thermal power much higher than that considered in the present work.

The CO and  $NO_x$  emissions reported above for the present combustor do not exceed 240 ppm and 46 ppm, respectively, for  $\alpha=50\%$  at both  $\lambda=1.5$  or  $\lambda=1.7$ , complying with the above-mentioned regulations. The CO emissions are too high for  $\lambda=1.3$  when secondary air is present. However, the emissions are lower than 42 ppm for CO and 65 ppm for  $NO_x$  when  $\lambda=1.3$  and  $\alpha=100\%$ , except in the case of pure hydrogen, where  $NO_x$  emissions reach 100 ppm.

Despite the beneficial influence of the secondary air for pure hydrogen, the combustor does not operate satisfactorily for mixtures of natural gas and hydrogen when  $\lambda=1.3$  and secondary air is present, owing to the high level of CO emissions arising from incomplete combustion. Even though gas turbine combustors typically operate with higher excess air, and the results obtained for  $\alpha=50\%$  at both  $\lambda=1.5$  or  $\lambda=1.7$  lead to low to moderate CO and  $NO_x$  emissions, there is room for improvement in the design of the combustor. The limited penetration of the secondary air jets suggests that increasing their injection momentum, e.g. reducing the diameter of the injection holes, or increasing the length of the top piece may allow for improved mixing and combustion, thereby reducing the CO emissions. Moreover, air preheating might allow operation under MILD conditions, which should further reduce  $NO_x$  emissions.

## Conclusions

An experimental investigation of the combustion of natural gas/hydrogen mixtures was conducted on a novel laboratory combustion system, where secondary air is injected towards the base through a plenum mounted at the top of a vertical combustor. The non-premixed flame

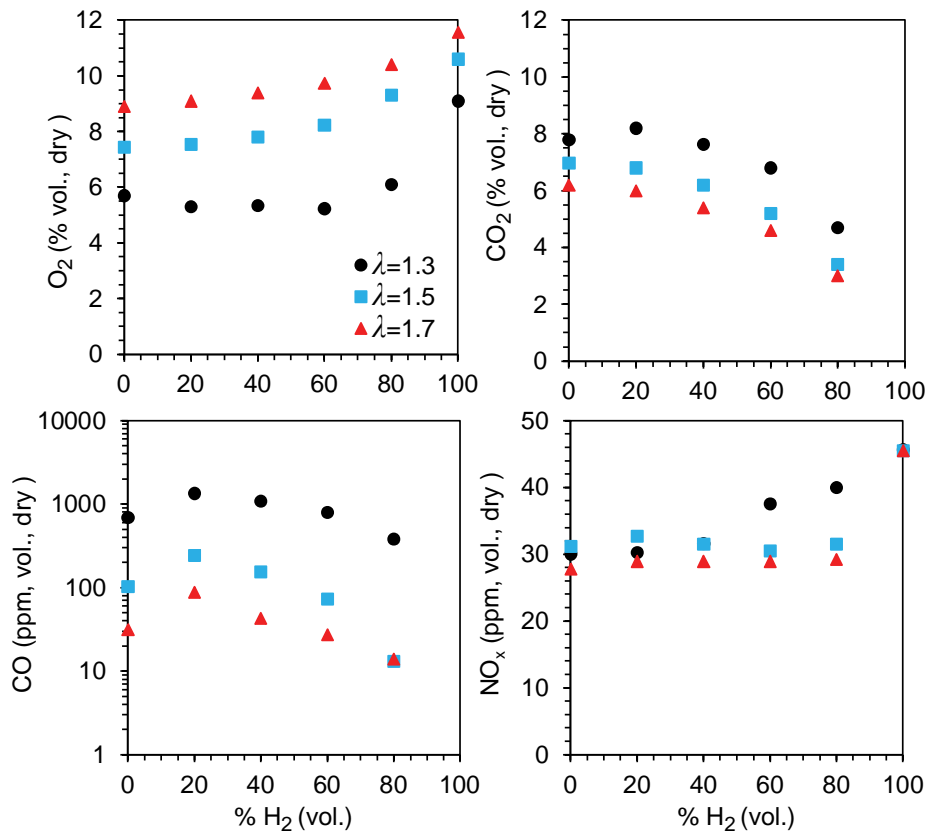


**Figure 5.** Molar fractions of the species at the exit for  $\alpha=50\%$  as a function of the percentage of hydrogen in the fuel and excess air coefficient.

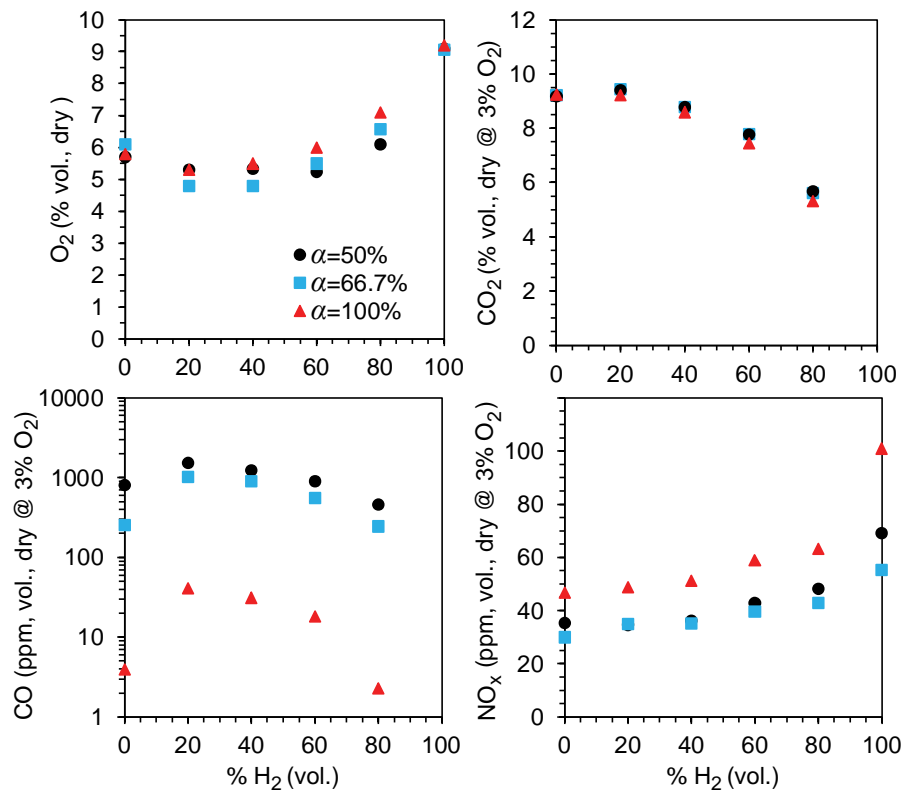


**Figure 6.** Molar fractions of the species at the exit for  $\lambda=1.3$  as a function of the percentage of hydrogen in the fuel and percentage of primary air.

was stabilised using a swirl burner. The influence of the amount of hydrogen in the fuel mixture (0%–100%), the fraction of primary air ( $\alpha=50\%$ –100%) and the excess air coefficient ( $\lambda=1.3$ –1.7) were studied. The following conclusions may be drawn from the analysis carried out:

- (i) The axial temperature profiles for natural gas/hydrogen mixtures containing 20% to 80% H<sub>2</sub> are relatively similar. However, as the hydrogen content in the mixture increases, the temperature rise near the burner slightly moves away from the burner. The profile for pure hydrogen, regardless of the values of  $\alpha$  and  $\lambda$ , is distinctly different, showing a higher temperature peak that occurs closer to the burner.
- (ii) Increasing the overall excess air results in a faster rise and a slight increase in the axial temperature, along with a small increase in the peak temperature, particularly when  $\lambda$  increases from 1.5 to 1.7.
- (iii) The temperature rises more rapidly downstream of the burner as the amount of primary air increases. The peak temperature occurs closer to the burner when  $\alpha = 100\%$ .
- (iv) When  $\lambda=1.3$  and secondary air is present, the CO emissions are excessively high for practical applications, indicating incomplete combustion. These emissions are significantly reduced with an increase in the excess air coefficient, a decrease in the percentage of secondary air, or when the hydrogen content in the fuel increases above 20%.
- (v) At  $\lambda=1.3$ , NO<sub>x</sub> emissions increase with hydrogen content. These emissions decrease slightly as  $\alpha$  rises from 50 to 66.7% but increase again at  $\alpha=100\%$ , peaking at about 100 ppm for pure hydrogen. At higher excess air coefficients, NO<sub>x</sub> emissions vary little with hydrogen content up to 80% but rise for pure hydrogen, although they do not exceed 50 ppm.
- (vi) The use of secondary air reduces NO<sub>x</sub> emissions but leads to an increase in CO emissions. Therefore, it is only beneficial when the excess air is sufficient to keep CO emissions within an acceptable range.

### Acknowledgements

The authors acknowledge Fundação para a Ciência e a Tecnologia (FCT) for its financial support via the projects no. 2022.08675.PTDC (<http://doi.org/10.54499/2022.08675.PTDC>) and LAETA Base Funding (DOI: 10.54499/UIDB/50022/2020). Gonçalo Pacheco acknowledges FCT for the provision of Scholarship 2021.04674.BD.

### References

- [1] *World Energy Outlook*, International Energy Agency (2004), <https://www.iea.org/reports/world-energy-outlook-2024> [accessed 16/11/2004].
- [2] Capurso, T., Stefanizzi, M., Torresi, M., Camporeale, S.M., “Perspective of the role of hydrogen in the 21st century energy transition”, *Energy Convers. Manage.* 251:114898 (2022).
- [3] Ishaq, H., Dincer, I., Crawford, C., “A review on hydrogen production and utilization: Challenges and opportunities”, *Int. J. Hydrogen Energy* 47:26238–26264 (2022).
- [4] Loprete, J., Hadlich, R.R., Sirna, A., Shaalan, A., Assanis, D., “Combustion Performance and Emissions Characterization of Methane-Hydrogen Blends (Up to 50% by Vol.) in a Spark-Ignited CFR Engine”, *Proc. Internal Combustion Engine Division Fall Technical Conference*, Pittsburgh, PA, paper ICEF2023-110538 (2023).
- [5] Colorado, A., McDonell, V., “Surface stabilized combustion technology: An experimental evaluation of the extent of its fuel flexibility and pollutant emissions using low and high calorific value fuels”, *Appl. Therm. Eng.* 136:206–218 (2018).

- [6] Hu E, Huang Z, He J, Jin C, Zheng J., “Experimental and numerical study on laminar burning characteristics of premixed methane–hydrogen–air flame”, *Int. J. Hydrogen Energy* 34:4876–4888 (2009).
- [7] Bothien, M.R., Ciani, A., Wood, J.P., Fruechtel, G., “Toward decarbonized power generation with gas turbines by using sequential combustion for burning hydrogen”, *J. Eng. Gas Turbines Power* 141:121013 (2019).
- [8] Wang, Y., Han, H.S., Sohn, C.H., “A comparative study of chemical-kinetic mechanisms for combustion of methane/hydrogen/air mixtures”, *Int. J. Aeron. Space Sci.* 25:519–539 (2024).
- [9] Ferrarotti, M., De Paepe, W., Parente, A., “Reactive structures and NO<sub>x</sub> emissions of methane/hydrogen mixtures in flameless combustion”, *Int. J. Hydrogen Energy*, 46:34018–34045 (2021).
- [10] Zhao, Y., McDonnell, V., Samuelsen, S., “Influence of hydrogen addition to pipeline natural gas on the combustion performance of a cooktop burner”, *Int. J. Hydrogen Energy* 44:12239–12253 (2019).
- [11] Kim, H.S., Arghode, V.K., Gupta, A.K., “Flame characteristics of hydrogen-enriched methane–air premixed swirling flames”, *Int. J. Hydrogen Energy* 34:1063–1073 (2009).
- [12] Kashir, B., Tabejamaat, S., Jalalatian, N., “A numerical study on combustion characteristics of blended methane-hydrogen bluff-body stabilized swirl diffusion flames”, *Int. J. Hydrogen Energy* 40:6243–6258 (2015).
- [13] Schefer, R.W., Wicksall, D.M., Agrawal, A.K., “Combustion of hydrogen-enriched methane in a lean premixed swirl-stabilized burner”, *Proc. Comb. Inst.* 29:843–851 (2002).
- [14] Kim, H.S., Arghode, V.K., Linck, M.B., Gupta, A.K., “Hydrogen addition effects in a confined swirl-stabilized methane-air flame”, *Int. J. Hydrogen Energy* 34:1054–1062 (2009).
- [15] Du, W., Zhou, S., Qiu, H., Zhao, J., Fan, Y., “Experiment and numerical study of the combustion behavior of hydrogen-blended natural gas in swirl burners”, *Case Stud. Therm. Eng.* 39:102468 (2022).
- [16] Elbayoumi, M., Garnier, F., Seers, P., “Numerical study of the impact of hydrogen addition, swirl intensity and equivalence ratio on methane-air combustion”, *Int. J. Turbo Jet Eng.*, 41:377–393 (2024).
- [17] Cozzi, F., Coghe, A., “Behavior of hydrogen-enriched non-premixed swirled natural gas flames”, *Int. J. Hydrogen Energy* 23:669–677 (2006).
- [18] Mokheimer, E.M.A., Sanusi, Y.S., Habib, M.A., “Numerical study of hydrogen-enriched methane–air combustion under ultra-lean conditions”, *Int. J. Energy Res.* 40:743–762 (2016).
- [19] Rajpara, P., Shah, R., Banerjee, J. “Effect of hydrogen addition on combustion and emission characteristics of methane fueled upward swirl can combustor”, *Int. J. Hydrogen Energy* 43:17505–17519 (2018).
- [20] Gee, A.J., Neil Smith b, Alfonso Chinnici a, Paul R. Medwell, “Characterisation of turbulent non-premixed hydrogen-blended flames in a scaled industrial low-swirl burner”, *Int. J. Hydrogen Energy* 49:747–757 (2024).
- [21] Daurer, G., Schwarz, S., Demuth, M., Gaber, C., Hochenauer, C., “Experimental and numerical analysis of industrial-type low-swirl combustion of hydrogen enriched natural gas including OH\* chemiluminescence imaging”, *Int. J. Hydrogen Energy* 80, 890–906 (2024).